Astron. Astrophys. 359, 799–810 (2000)

ASTRONOMY AND ASTROPHYSICS

Condensation and growth of hydrogenated carbon clusters in carbon-rich stars

G. Pascoli and A. Polleux

Faculté des Sciences, Département de Physique, 33 rue Saint Leu, 80039 Amiens Cedex, France

Received 22 September 1999 / Accepted 28 February 2000

Abstract. Hydrogenated carbon cluster growth in carbon-rich stellar atmospheres is simulated by a model which takes into account the simultaneous formation of carbon compounds with carbon atoms under various states of hybridization. A grid of computations shows that a mixture of different species can appear (small hydrogenated carbon clusters, carbon chains or ring-shaped structures, aromatic-like entities, etc.) depending on both carbon to hydrogen relative abundance and temperature of the star. Dehydrogenation rate and sp2/sp and sp3/sp ratios are estimated.

Key words: molecular processes – stars: circumstellar matter – ISM: general – ISM: molecules

1. Introduction

The chemistry and physics of carbon clusters have long been recognized as being extremely important in such diverse applied fields as heterogeneous catalysis and soot formation during combustion. More recently new technological areas have developed which focus on fullerene chemistry (Kroto et al. 1985; Weltner & Van Zee 1989; Krätschmer et al. 1990; Fye & Jarrold 1997). Since carbon clusters have been identified in interstellar and circumstellar media by radiowave or infrared spectroscopy, this topic has also attracted considerable interest in astrophysics (see Williams 1994 for a review). Among these carbon clusters many of them are found to be small in size, possessing only three or four atoms (Omont 1993). However medium-sized species also exist appearing in the form of an archetypical cumulenic or acetylenic carbon chain, C_n, with one or two foreign atoms such as H or N attached to the extremities (Cherchneff et al. 1993; Cherchneff 1995). In contrast to these nanoscopic structures, the presence of microscopic entities such as carbonaceous grains has long been attested, in circumstellar envelopes surrounding cool giant stars, by IR absorption and emission (Merrill 1977). Dust grains have been thus invoked in driven mass loss in these stars during late stages of their evolution (Kwok 1975; Tielens 1983). Following a classical scenario, grains acquire momentum from stellar radiation field and collisions with gas eventually eject mass at a higher rate in space (Knapp 1986). However, in order that this mechanism be really efficient, grains must form in the vicinity of the star, namely in a region located above the photosphere and over a distance not exceeding a few stellar radii (Sedlmayr 1990). Thus one of the major problems for the astrochemists relates to understanding better the chemical pathways towards microscopic structures (like carbonaceous grains composed of thousands of atoms) starting from very small radicalar clusters (such as C_2, C_3, C_2H or C_3H) [A very similar problem can be seen in oxygen-rich stars but with formation of silicate grains (Tielens 1990)]. A second important point is that the structure of the interstellar and circumstellar medium-sized clusters is still largely unknown. Many candidates have been postulated such as polycyclic aromatic hydrocarbons (hereafter referred as PAHs) (Tielens 1993), fullerenes (Krätschmer 1993), but also carbynes, i.e. long carbon chains and monocyclic rings (Thaddeus 1994). PAHs are thought to be quite abundant and ubiquitous in the outer region of circumstellar envelopes and in interstellar medium (Léger & Puget 1984). Allamandola et al. (1989) concluded that interstellar PAHs should be singled ionized and estimated their carbon atom numbers to be in the range 20 to 200. A similar conclusion that interstellar PAHs are ionized and partially dehydrogenated due to the UV interstellar fields is made by Allain et al. (1996a,b). Various authors have shown that PAHs can be produced directly in situ via a complex circumstellar or interstellar chemistry (Herbst 1991; Tielens 1993) or can also originate from carbon star atmospheres (Cherchneff et al. 1992; Cadwell et al. 1994; Cherchneff 1995). In any case, the physical conditions prevailing in the region where these clusters are formed have to play an important role and, possibly, other more exotic species such as carbynes and fullerenes may exist as well. We can see that spectra of true (fully hydrogenated) PAHs in both neutral and cationic forms have been clearly identified by the experimentalists (Léger & Puget 1984; Salama & Allamandola 1993). Besides, only a few experimental studies have been devoted to carbyne spectra (Freivogel et al. 1995). Accordingly, the assignment of the so-called diffuse interstellar bands (DIBs) observed in circumstellar and interstellar media to either aromatic-like species (PAHs ionized or not, partially or strongly dehydrogenated), carbon chains or monocycles still remains an open debate (Kerr et al. 1996). The matter is especially complex given that the different forms of carbon enumerated above can, potentially, coexist in various proportions in space. In this paper, we are only concerned with aggregation and growth of

carbon clusters in a carbon-rich stellar atmosphere. We are not restricted to a special class of clusters such as PAHs or carbynes but rather our aim is to simultaneously consider the three possible types of hybridization for carbons, i.e. sp (alkynes), sp2 (alkenes and aromatic structures) and sp3 (alkanes, branched or not). In addition to these standard species, dehydrogenated structures with dangling bonds (radicalar clusters) have been considered. Estimates of sp2/sp and sp3/sp ratios are given, together with dehydrogenation rates for the various compounds. The limiting action on cluster growth due to both photodetachment of small radicalar entities or saturation of dangling bonds by hydrogen is also analysed.

2. Methods

Between nanoscopic carbon clusters such as C_2, C_2H, C_3, etc. and microscopic carbonaceous grains different kinds of medium-sized hydrocarbons may exist. In the present study, we only consider

i/ aromatic molecules (2D structures) in which the C atoms are sp2-hybridized. As a very typical example, we can cite the PAHs.

ii/standard alkanes, alkenes and alkynes.

iii/ the preceding structures i/ and ii/ but in various states of dehydrogenation. The different species are then labelled "species-like" (Fig. 1). For total dehydrogenation of chains with a number of carbon atoms larger than 10, pure carbon monocyclic rings are assumed to be the ground state geometry (Weltner & Van Zee 1989) and fullerenes when $n \geq 60$ (Hunter et al. 1994) [note that for pure carbon clusters with heteroatoms belonging to the first and second rows of the periodic table, it has been found that the closure of the chain in a monocyclic ring is delayed at values of n larger than 10 (Pascoli & Lavendy 1998a,b), but we do not consider this case here]. In fact, for each species, a large number of isomers can be present in a metastable state [For instance the linear chains can coexist with monocycles when $10 \leq n \leq 60$ and with fullerenes when $N \geq 60$, Fye & Jarrold 1997)]. Finally intermediary forms for the chains can also exist, given their floppiness. The energetic separations between all these intermediary forms can be smaller than 1–2 eV and one form can pass to another one in the ambient radiation field.

The way all the different types of structures i/, ii/, iii/ are built when competition exists between them, has not yet been examined even though this point appears to be very important to understand the nucleation process of growth of carbon clusters in diluted media (for instance, in carbon-rich stellar atmospheres). In the following, (N, P) designates a cluster with N carbons and P hydrogens. The corresponding abundances are denoted $[N, P]$. For instance, when a cluster (N, P) captures a carbon atom, it becomes the cluster $(N + 1, P)$. The relative velocity, v, between the carbon atom and the cluster (N, P) is assumed to be determined by the Maxwell-Boltzmann statistics.

Table 1. Fragments for each type of compounds

type	fragments						
alkane-like	C	H	CH	CH_2	CH_3		
alkene-like	C	H	CH	CH_2			
alkyne-like	C	H	CH	C_2H	C_3H	C_2	C_3
aromatic-like	C	H	CH	CH_2	C_2H_2		

The effective cross-section, $\langle\sigma\rangle$, for addition of a carbon atom to a (N, P) cluster is given by

$$\langle\sigma\rangle = \frac{\langle\sigma v\rangle}{v_{\rm C}} = \frac{\int_0^\infty \sigma v F(v)\,{\rm d}v}{v_{\rm C}} \tag{1}$$

where

$$F(v)\,{\rm d}v = \frac{4}{\sqrt{\pi}}\left(\frac{v}{v_{\rm C}}\right)^2 \exp\left[-\left(\frac{v}{v_{\rm C}}\right)^2\right]\frac{{\rm d}v}{v_{\rm C}} \tag{2}$$

with the most probable relative velocity

$$v_{\rm C}(N,P) = \left(\frac{2kT}{\mu_{\rm C}(N,P)}\right)^{1/2}. \tag{3}$$

In the latter expression, T designates the gas temperature and $\mu_{\rm C}(N,P) = \frac{m_{\rm C}(Nm_{\rm C}+Pm_{\rm H})}{(N+1)m_{\rm C}+Pm_{\rm H}}$, the reduced carbon mass.

Similar relations are used for addition of a hydrogen atom to all species or, more specifically, a C_2 or a C_2H radical to alkyne-like species. The aggregation process by addition of a C or H atom, a C_2 or C_2H radical is limited by opposite mechanisms of chemical attack or photodestruction due to radiation field. Fragments produced by photodissociation are listed in Table 1. We assume that the star radiates as a black body at temperature T_*.

The mean field equation governing the change in density of any cluster (N, P), with time is

$$\begin{aligned}
&\frac{{\rm d}[N,P]}{{\rm d}t} \\
&= K_{\rm C}(N-1,P)[1,0][N-1,P] \\
&\quad + K_{\rm H}(N,P-1)[0,1][N,P-1] \\
&\quad + K_{\rm C_2}(N-2,P)[2,0][N-2,P] \\
&\quad + K_{\rm C_2H}(N-2,P-1)[2,1][N-2,P-1] \\
&\quad + K_{\rm H}^{\rm stripping}(N,P+1)[0,1][N,P+1] \\
&\quad - K_{\rm C}(N,P)[1,0][N,P] \\
&\quad - K_{\rm H}(N,P)[0,1][N,P] \\
&\quad - K_{\rm H}^{\rm stripping}(N,P)[0,1][N,P] \\
&\quad - K_{\rm C_2}(N,P)[2,0][N,P] - K_{\rm C_2H}(N,P)[2,1][N,P] \\
&\quad + \sum_{\{i,j\}} K^{\rm diss}(N+i,P+j\rightarrow N,P)[N+i,P+j] \\
&\quad - \sum_{\{i,j\}} K^{\rm diss}(N,P\rightarrow N-i,P-j)[N,P]
\end{aligned} \tag{4}$$

When $N \leq 4$, however, the whole set of reactions tabulated by Baulch et al. (1992), involving small hydrogenated carbon

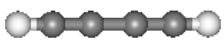

standard alkyne

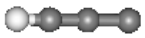

alkyne-like
starting geometry : corresponding standard alkyne with CH extracted

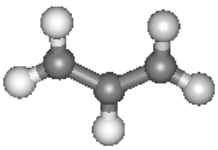

standard alkene (1)

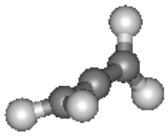

alkene-like (1)
starting geometry : corresponding standard alkene (1) with H extracted

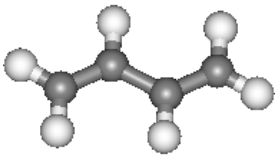

standard alkene (2)

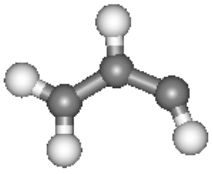

alkene-like (2)
starting geometry : corresponding standard alkene (2) with CH_2 extracted

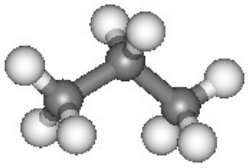

standard alkane

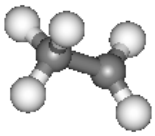

alkane-like
starting geometry : corresponding standard alkane with CH_3 extracted

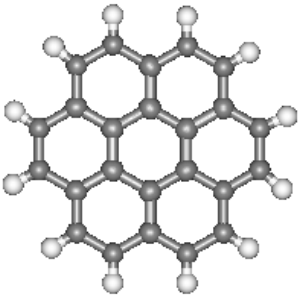

standard aromatic

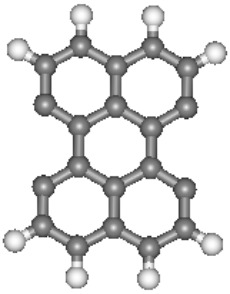

aromatic-like
starting geometry : corresponding standard aromatic with 2 C_2H_2 symmetrically extracted

Fig. 1. A sample of hydrogenated carbon clusters considered in this study.

clusters or radicals without heteroatoms, has also been incorporated.

The summations are over reactions which either create $(+)$ or destroy $(-)$ the species (N, P). These equations are not independent and are linked by the following conservation equations

$$\sum_{N,P}[N,P]N \;=\; n_{\rm C}$$

$$\sum_{N,P}[N,P]P \;=\; n_{\rm H} \qquad (5)$$

where $n_{\rm C}$ and $n_{\rm H}$ are the total number of carbon and hydrogen atoms, respectively (the summations are performed on all the species considered).

For a given (N, P), the second member of Eq. (4) includes the sticking of a carbon or a hydrogen atom, represented respectively by the first and second terms, the sticking of a $\rm C_2$

Table 2a. Mean geometrical areas for alkane, alkene, alkyne-like and aromatic-like compounds. N represents the number of carbon atoms in the structure and N_X the number of closed rings

species		$\sigma(N)$	a (Å)
alkyne-like[a]	$a \leq N$	$\frac{a^2}{3}(2N+\pi)$	1.27
alkene-like	$2 \leq N \leq 5$	[b]	—
alkane-like	$2 \leq N \leq 5$	[b]	—
aromatic-like	$N_X \geq 1$	$2a^2 N_X$	1.40
diamond-like	$N \geq 6$	$a^2 N^{2/3}$	1.54

[a] reduced by a factor 10 for $C_2 + C \rightarrow C_3$ and $C_2H + C \rightarrow C_3H$
[b] deduced from reactions tabulated by Baulch et al. (1992)

Table 2b. Relative probability, $\mu(N,P)$, of sticking of a hydrogen or carbon atom or any other small radicals to the coumpound (N,P)

type (non-branched)	$\mu(N,P)$
alkyne-like	
$P \leq 2$	$1 - \frac{P}{2}$
alkene-like	
$N \leq 5$[a]; $N+2 \geq P \geq 3$	$1 - \frac{P}{N+2}$
alkane-like	
$N \leq 5$[b]; $2N+2 \geq P \geq N+3$	$1 - \frac{P}{2N+2}$

[a] when $N \geq 6$, aromatic-like species are considered.
[b] when $N \geq 6$, branched structures (diamond-like) are assumed.

or C_2H radical to alkyne-like clusters (respectively third and fourth terms). Chemical attack by hydrogen atoms of hydrogenated clusters, which can be important at higher temperatures, is also taken into account for all species (fifth term) (except for alkyne-like species for which abstraction of H by this process is much more difficult to realize). A mean activation barrier of 0.7 eV has been adopted for stripping (see Kiefer et al. 1985; Frenklach & Feigelson 1989). The photodissociation of a C, H, CH_n ($n = 1-3$) or C_2H_2 group is represented by the eleventh term. The kernels $K_C(N-1,P)$, $K_H(N,P-1)$, $K_{C_2}(N-2,P)$ and $K_{C_2H}(N-2,P-1)$ represent respectively the probabilities of aggregation of C, H, C_2, C_2H; likewise $K^{\rm stripping}(N,P+1)$ denotes the probability of stripping and $K^{\rm diss}(N+i,P+j \rightarrow N,P)$ the probability of photodissociation relative to the reaction $N+i, P+j \rightarrow N,P$.

The kernels K_C, K_H, K_{C_2} and K_{C_2H} can be written in the form

$$K = \langle\sigma\rangle\, V \tag{6}$$

where V is defined by expressions similar to (3) for addition of H, C_2 and C_2H.

The determination of the quantity $\langle\sigma\rangle$ is a rather difficult task for any type of molecule-molecule reaction. However, reactions between radicalar compounds are exothermic and therefore not very temperature dependent. We can thus assume that $\langle\sigma\rangle$ is independent of T for each reagent cluster and can be written in the form

$$\langle\sigma\rangle = \mu(N,P)\sigma(N) \tag{7}$$

where $\sigma(N)$ is the mean geometrical area of the clusters with a skeleton composed of N carbons (Table 2a). The coefficients $\mu(N,P)$ indicate if addition of a hydrogen, a carbon atom or any other radicals is possible by testing the number of dangling bonds present in the structure (Table 2b). Similar relations to (6) and (7) for stripping reactions are used but i/ the coefficients $\mu(N,P)$ are taken from Table 3 (in order this time to ensure that no stripping can occur for fully dehydrogenated species, ii/ the expression (7) is multiplied by an activation factor written, as usual, in the form $\exp - \left(\frac{\Delta E}{kT}\right)$ with ΔE =0.7 eV (see above). In addition to radicalar reactions listed above, some important reactions, but which proceed with an activation barrier, have been also included for aromatic species. Formation of benzene by cyclotrimerization reactions of acetylene has been considered, but as is well known, we found this reaction is not efficient – or rather, benzene formation by this pathway requires a time prohibitively longer than the dynamic time scale for stellar wind [In fact the catalytic action of Fe could possibly lower this barrier, but this reaction is not easy to quantify, see Schröder et al. 1991]. A much more prominent – and low-energy – route to obtain a benzene ring is to go from the linear C_6 structure (which forms abundantly from linear clusters $C_{n<6}$) to the corresponding cyclic isomer (fully dehydrogenated benzenic ring). DFT calculations give a smaller value of 1.11 eV for the activation barrier for conversion of the C_6 linear into the cyclic form. On the other hand subsequent contamination by hydrogen stabilizes the cycle with creation of sp2 sites. This important route is also included in the present calculations [This pathway could also be envisaged for linear C_{10} which easily isomerizes into a fully dehydrogenated naphtalene-like structures, the latter ones being next stabilized by sticking of hydrogen atoms]. Starting from a benzenic ring, dual process with consecutive addition of C_4H_2 and C_2 to PAHs (activation barrier 1.85 eV) is also relevant (Stein 1978). The latter reaction is efficient for production of naphtalene from benzene due to the high abundance of diacetylene found in all cases. Moreover, its relative inefficiency for larger PAHs is due to the fact that free C_2 (or C_2H) is rapidly locked in the carbon chains and photofragmentation of this radical from these chains is not easy. Another possibility (not considered here) would be to add uniquely C_4H_2, but this route leads to a sequence of non compact structures, such as polyhelicene or polyacene components which are seemingly absent from the interstellar infrared emission spectra (Léger et al. 1989) [Conversely, an excess of C_2 radicals could lead from a seed of naphtalene to acenaphthylene with a five-membered ring and subsequently to a sequence of curved structures].

The photodestruction rate $K^{\rm diss}(N+i,P+j \rightarrow N,P)$ corresponding to the reaction $(N+i,P+j \rightarrow N,P)$ is given by

$$\begin{aligned} &K^{\rm diss}(N+i,P+j \rightarrow N,P) \\ &= \int_{\frac{E_{Di,j}(N,P)}{h}}^{\infty} \sigma_\nu(N+i,P+j \rightarrow N,P) \\ &\qquad \Phi_\nu(N+i,P+j \rightarrow N,P)\,{\rm d}\nu \end{aligned} \tag{8}$$

Table 3. Relative probability, $\mu_{i,j}(N,P)$, of photodetachment of a functional group (i,j) from the compound (N,P).

type (non-branched)	i,j	$\mu_{i,j}(N,P)$
alkyne-like	$1,0$; $2,0$; $3,0$	$1-\frac{P}{2}$
$P \leq 2$	$0,1$; $1,1$; $2,1$; $3,1$	$\frac{P}{2}$
alkene-like	$1,0$	$1-\frac{P}{N+1}$; $P \leq N+1$
$N+2 \geq P \geq 3$;	$1,1$	$\frac{4P}{N+2}\left(1-\frac{P}{N+2}\right)$
$N \leq 5$[a]	$0,1$; $1,2$	$\frac{P}{N+2}$
alkane-like	$1,0$	$1-\frac{P}{2N}$; $P \leq 2N$
$2N+2 \geq P \geq N+3$;	$1,1$	$\frac{4P}{2N+1}\left(1-\frac{P}{2N+1}\right)$; $P \leq 2N+1$
$N \leq 5$[b]	$1,2$	$\frac{4P}{2N+2}\left(1-\frac{P}{2N+2}\right)$
	$0,1$; $1,3$	$\frac{P}{2N+2}$

[a] When $N \geq 6$ and $P \geq 3$, aromatic-like species are favored over alkene-like structures. For aromatic-like entities the coefficients μ are determined separately in each individual case and no analytic expression is given.
[b] When $N \geq 6$ and $P \geq N+3$, alkanes are assumed to exist in compact form. As for aromatic-like species, the coefficients μ are separately determined in each individual case.

where σ_ν is the absorption cross section (cm^2) and Φ_ν is the emittance of photons at frequency ν (cm^{-2}s^{-1}Hz^{-1}). Quantum efficiency is taken equal to the unity. The limit of integration, $\frac{E_{Di,j}(N,P)}{h}$, represents the threshold frequency, directly expressed as a function of the dissociation energy $E_{Di,j}(N,P)$. The latter quantity is the minimal energy required to dissociate the cluster $(N+i,P+j)$ into the cluster (N,P) and a fragment (i,j). At $r=r_*$, the photon distribution law is given by the Planck function (Allen 1963): $\Phi_\nu = \frac{2\pi}{c^2}\frac{\nu^2}{\left(\exp\left(\frac{h\nu}{kT_*}\right)-1\right)}$. The amount of radiation which is absorbed and re-emitted at IR wavelengths as due to the photodissociation reaction $N+i,P+j \rightarrow N,P$ can be expressed as follows

$$\frac{\mathrm{d}}{\mathrm{d}t}\Phi_\nu = -\sigma_\nu \Phi_\nu [N+i,P+j]c. \quad (9)$$

Absorption of UV radiation by elements having a low ionization potential and a relatively high fractional abundance, namely Na (I.P. = 5.14 eV), Mg (I.P. = 7.64 eV), Al (I.P. = 5.98 eV), Ca (I.P. = 6.11 eV) and Fe (7.90 eV) has also been taken into account. Photoabsorption cross-sections for these elements in the energy range 5–7 eV are adapted from calculations performed by Reilman & Manson (1979).

Eventually, a extra factor is included for geometrical dilution of radiation at distances larger than r_*. In the mean field approximation, we can write

$$K^{\mathrm{diss}} = \sigma(N)\mu_{i,j}(N,P)\Phi(E_{\mathrm{diss}},T_*) \quad (10)$$

The coefficients $\mu_{i,j}(N,P)$ represent the relative probabilities of photodetachment of a functional group (i,j) from the compound $(N+i,P+j)$. These quantities are listed in Table 3 for alkane-like, alkene-like and alkyne-like species. The geometrical cross sections, $\sigma(N)$, are defined above. At $r=r_*$, we have $\Phi(E_{\mathrm{diss}},T_*) = \int_{\frac{E_{\mathrm{diss}}}{h}}^{\infty} \frac{2\pi}{c^2}\frac{\nu^2}{\left(\exp\left(\frac{h\nu}{kT_*}\right)-1\right)}\,\mathrm{d}\nu$.

The energetics of the various photodestruction reactions is determined by the dissociation energies $E_{Di,j}(N,P)$ (Table 4). These parameters were computed employing the package GAUSSIAN94 (Frisch at al. 1995). Density functional theory with B3LYP functional has been chosen. For each species, i.e. each couple (N,P), a number of structures have been optimized in order to determine

i/ the ground state geometry for given N and P.

ii/ the dissociation energy of any functional group belonging to the series listed in Table 1.

These operations were carried out for a number of species and fits have been derived for the other neighbouring congeners (Figs. 2, 3). In fact, many isomers exist for each species

Table 4. Dissociation energies, E_{D} (eV), for a few typical reactions calculated with DFT/B3LYP method (Frisch et al. 1995)

	E_{D} (eV)
alkyne-like	
$C_3H_2 \rightarrow C_3H + H$	4.35
$C_5H_2 \rightarrow C_2H + C_3H$	6.31
$C_7H \rightarrow C_4H + C_3$	5.71
alkene-like	
$CH_2 \rightarrow CH + H$	4.38
$C_3H_4 \rightarrow C_3H_3 + H$	2.15
$C_3H_5 \rightarrow C_2H_3 + CH_2$	5.93
$C_3H_5 \rightarrow C_3H_4 + H$	2.80
$C_4H_6 \rightarrow C_4H_5 + H$	5.12
alkane-like	
$C_2H_6 \rightarrow 2CH_3$	4.19
$C_2H_6 \rightarrow C_2H_5 + H$	4.68
$C_3H_7 \rightarrow C_2H_5 + CH_2$	4.68
$C_3H_8 \rightarrow C_3H_7 + H$	4.71
$C_3H_8 \rightarrow C_2H_5 + CH_3$	4.03
aromatic-like	
$C_6H_6 \rightarrow C_6H_5 + H$	5.03
$C_{10}H_8 \rightarrow C_8H_6 + C_2H_2$	7.65
$C_{24}H_{12} \rightarrow C_{20}H_8 + 2C_2H_2$	7.97

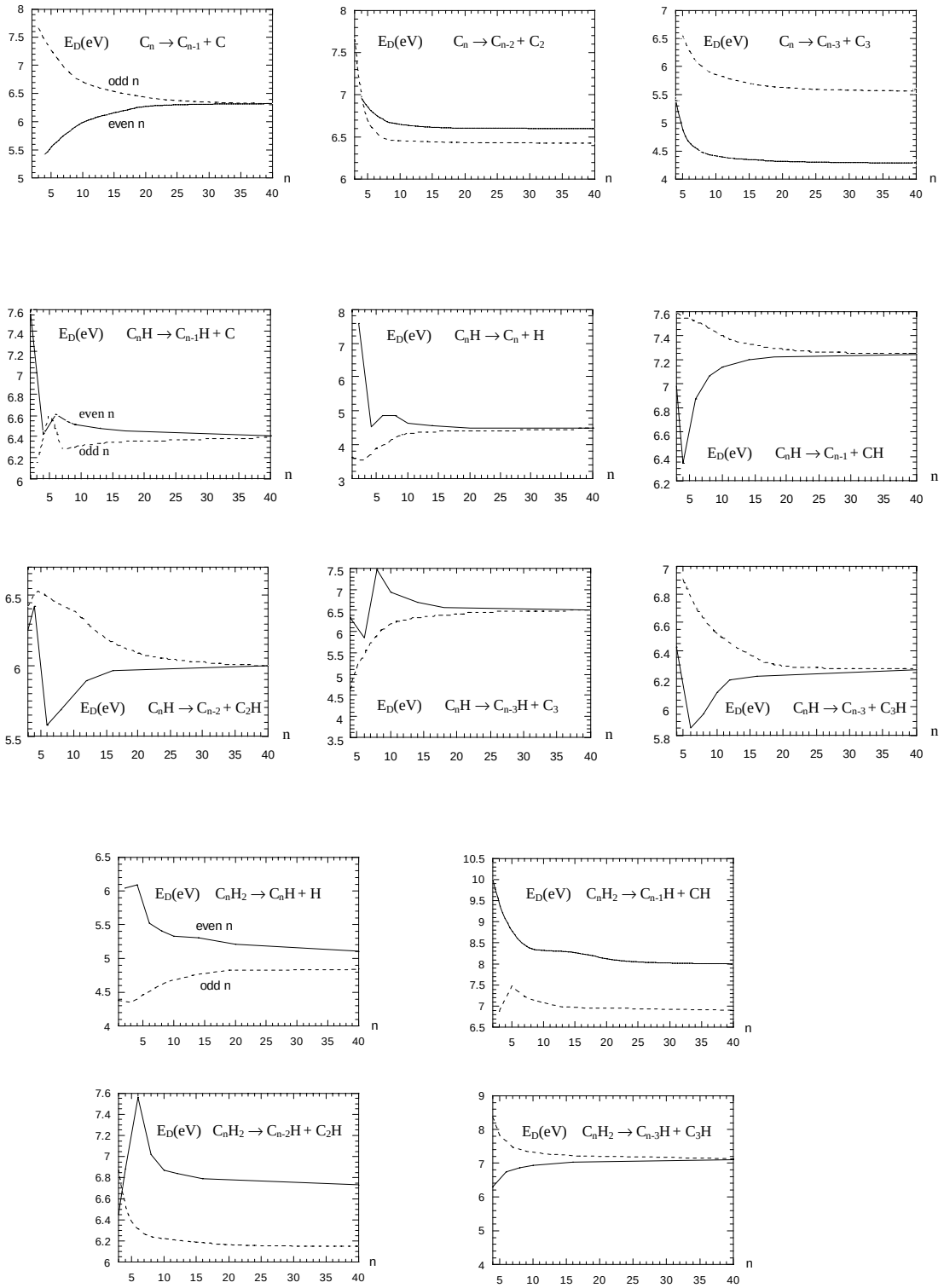

Fig. 2. Dissociation energies plotted as functions of N (number of carbon atoms) for the reactions $(N+i, P+j) \rightarrow (N,P) + (i,j)$ in alkyne-like structures.

(N,P) and very often the energetic separations between them are smaller than 1–2 eV. In particular, the carbon chains appear very floppy and can easily pass from a perfect linear form to a strongly bent or a (mono- or poly-) cyclic structure (Weltner & Van Zee 1989). The coexistence of many (metastable) isomers is possible in the gas. For instance, the cyclic geometry is favored for C_{10}, but this form can coexist with other isomeric configurations such as the linear geometry, the fully dehydrogenated naphtalene, the fully dehydrogenated azulene, etc., under various proportions following the energetics of these

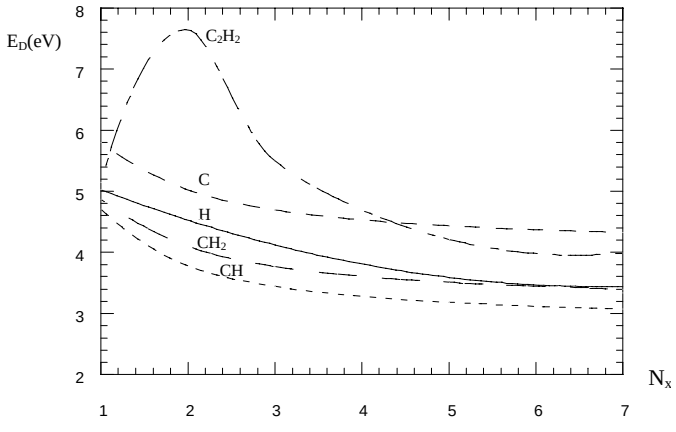

Fig. 3. Dissociation energies plotted as functions of N_X (number of aromatic cycles) for the reactions $(N+i, P+j) \rightarrow (N,P)+(i,j)$ in aromatic-like structures.

species; even though the presence of hydrogen preferentially stabilizes the polycyclic forms. Nevertheless, here, the dissociation energies are computed for species in the ground state configuration. For aromatic-like compounds, a similar procedure was carried out even though the situation is more complex. Computations show that, for given N and P, compact forms are preferred. In the case of complete aromatic clusters composed of closed rings (PAHs), we have selected two possiblities: i/ photodetachment of a hydrogen atom ii/ photoframentation of a C_2H_2 group (acetylene). For incomplete clusters, three possibilities are envisaged: i/ photodetachment of a hydrogen atom, a CH or CH_2 radical, iii/ photodetachment of a carbon atom when the latter one is in a free position, i.e. when a carbon atom is attached to the main structure by only one bond. Finally, the set of Eqs. (4) and (9) has been solved for a stellar wind with standard mass loss rate, $\dot{M} \sim 10^{-5}$ solar mass by year. Constant expansion velocity, $v_e \sim 10$ km/s, and spherical symmetry with adiabatic cooling for the gas ejection, are likewise assumed for simplification (Habing 1996); even though in the vicinity of the stellar surface turbulence and, possibly magnetic field, can produce very intricate gas motions (Pascoli 1997).

3. Results and discussion

Condensation and growth of about one thousand different species have been simulated. Various regimes of temperature T_* = 2000, 3000, 5000 and 7000 K have been considered for three carbon to hydrogen abundance ratios $\frac{n_C}{n_H} = 10^{-1}$ ($n_H = 10^{12}\mathrm{cm}^{-3}$), 1 ($n_H = 10^{11}\mathrm{cm}^{-3}$) and 10 ($n_H = 10^{11}\mathrm{cm}^{-3}$). Results of these calculations are displayed in Figs. 4–10. Other cases with relative abundance ratios smaller than (or equal to) 10^{-2} have been also considered, but are not presented here. In fact, for weak values of this ratio, only very small clusters are created. For instance, at $T_* = 2000$ K and for $\frac{n_C}{n_C} = 10^{-2}$, hydrogen is essentially in its molecular form and carbon is locked in C_2H_2. The longest carbon chain is C_4H_2 with a relative abundance of 10^{-7}. A comparison with relative abundance of C_4 (10^{-14}), clearly indicates that hydrogenation of C_4 prohibits the formation of chains with $n \geq 4$. Benzene is formed at an insignificant rate and consequently aromatic-like species are absent.

A/ $T_* = 2000$–$3000\,K$

For higher carbon to hydrogen ratio, the situation is quite different and much more interesting. However in the following, in order to convey the discussion more directly, we essentially discuss the model with $\frac{n_C}{n_H} = 1$. Other modeling results are given but by way of comparison. For stellar temperature $T_* = 2000$ K and $\frac{n_C}{n_H} = 1$, the $[\frac{C_3}{C_2}]$ ratio is very high, $\sim 10^3$, due to the fact that i/ C_2 is fully hydrogenated in C_2H_2 ($[\frac{C_2H_2}{C_2}] \sim 10^3$ whereas $[\frac{C_3H_2}{C_3}] \sim 1$), ii/ C_3 is more easily photofragmented from the carbon chains than C_2. Cyclopropenylidene (C_3H_2) and diacetylene (C_4H_2) are among the most important species: $[C_3H_2] \sim 10^{-2}$, $[C_4H_2] \sim 10^{-2}$ – 10^{-3}. The chains C_nH and C_nH_2 are indeed abundant up to $n = 30$ (Fig. 8), $[\frac{C_{30}H}{C_3}] \sim 10^{-2}$ (resp. $\sim 4\,10^{-5}$ for $\frac{n_C}{n_H} = 0.1$ and $\sim 3\,10^{-3}$ for $\frac{n_C}{n_H} = 10$), $[\frac{C_{30}H_2}{C_3}] \sim 5\,10^{-3}$ (resp. $\sim 10^{-5}$ for $\frac{n_C}{n_H} = 0.1$ and $\sim 8\,10^{-3}$ for $\frac{n_C}{n_H} = 10$). However very large chains with $n \geq 60$ are also present, though in smaller proportions (Fig. 8), $[\frac{C_{60}H}{C_3}] \sim 10^{-4}$ (respectively $\sim 10^{-9}$ for $\frac{n_C}{n_H} = 0.1$ and $\sim 3\,10^{-4}$ for $\frac{n_C}{n_H} = 10$), $[\frac{C_{60}H_2}{C_3}] \sim 10^{-5}$ (respectively $\sim 10^{-8}$ for $\frac{n_C}{n_H} = 0.1$ and $\sim 7\,10^{-5}$ for $\frac{n_C}{n_H} = 10$). For pure carbon monocyclic structures ($n \geq 10$), we obtain $[\frac{C_{10}}{C_3}] \sim 5\,10^{-3}$ (respectively $\sim 10^{-7}$ for $\frac{n_C}{n_H} = 0.1$ and $\sim 10^{-2}$ for $\frac{n_C}{n_H} = 10$) and $[\frac{C_{60}}{C_3}] \sim 10^{-3}$ (respectively $\sim 10^{-9}$ for $\frac{n_C}{n_H} = 0.1$ and $\sim 10^{-2}$ for $\frac{n_C}{n_H} = 10$). As described by Hunter et al. (1994), carbon chains with $n \geq 60$ are very floppy and can eventually lead to rigid polyhedral structures, such as fullerenes by structural rearrangement (note in particular the Fig. 7 displayed in their paper). With reference to fullerenes, we suggest another route leading to curved or spheroidal structures by direct association and reprocessing of C_{10} rings (Goeres & Sedlmayr 1991), the latter species being indeed found abundantly in the present model ($[C_{10}] \sim 10^{-4}$). Total abundance of linear clusters with a number of carbon atoms, N, larger than 60 relatively to total abundance of linear and ring-shaped clusters with $n < 60$, that is $\frac{\sum(N \geq 60)}{\sum(N<60)}$, is of the order of 10^{-2}, which indicates that production of fullerenes can be appreciable, even though linear chains and rings are clearly dominant. Rate of benzene is found to be high, $[\frac{C_6H_6}{C_2H_2}] \sim 2\,10^{-2}$, and relative abundance of naphtalene with respect to benzene is equally high, $[\frac{C_{10}H_8}{C_6H_6}] \sim 0.2$. These aromatic species are slightly dehydrogenated, $[\frac{C_6H_5}{C_6H_6}] \sim 10^{-3}$, $[\frac{C_{10}H_7}{C_{10}H_8}] \sim 0.02$. Thus small PAHs are only partially stripped of their hydrogens. On the other hand aromatic-like compounds with functional groups attached to them appear fairly abundant, $[\frac{C_6H_5-CH_2}{C_6H_6}] \sim 0.4$, $[\frac{C_6H_5-CH-CH_2}{C_6H_6}] \sim 0.2$. Besides, for the coronene, we have $[\frac{C_{24}H_{12}}{C_6H_6}] \sim 10^{-9}$ (Fig. 9a). In fact, the latter species appears in a highly dehydrogenated state, $[\frac{C_{24}H_6}{C_{24}H_{12}}] \sim 10^4$ (Fig. 9b) [except when the carbon to hydrogen ratio is smaller than unity, for $\frac{n_C}{n_H} = 0.1$ we find $[\frac{C_{24}H_6}{C_{24}H_{12}}] \sim 10^{-2}$]. As a general rule, larger PAHs are fully dehydrogenated, i.e. appear in

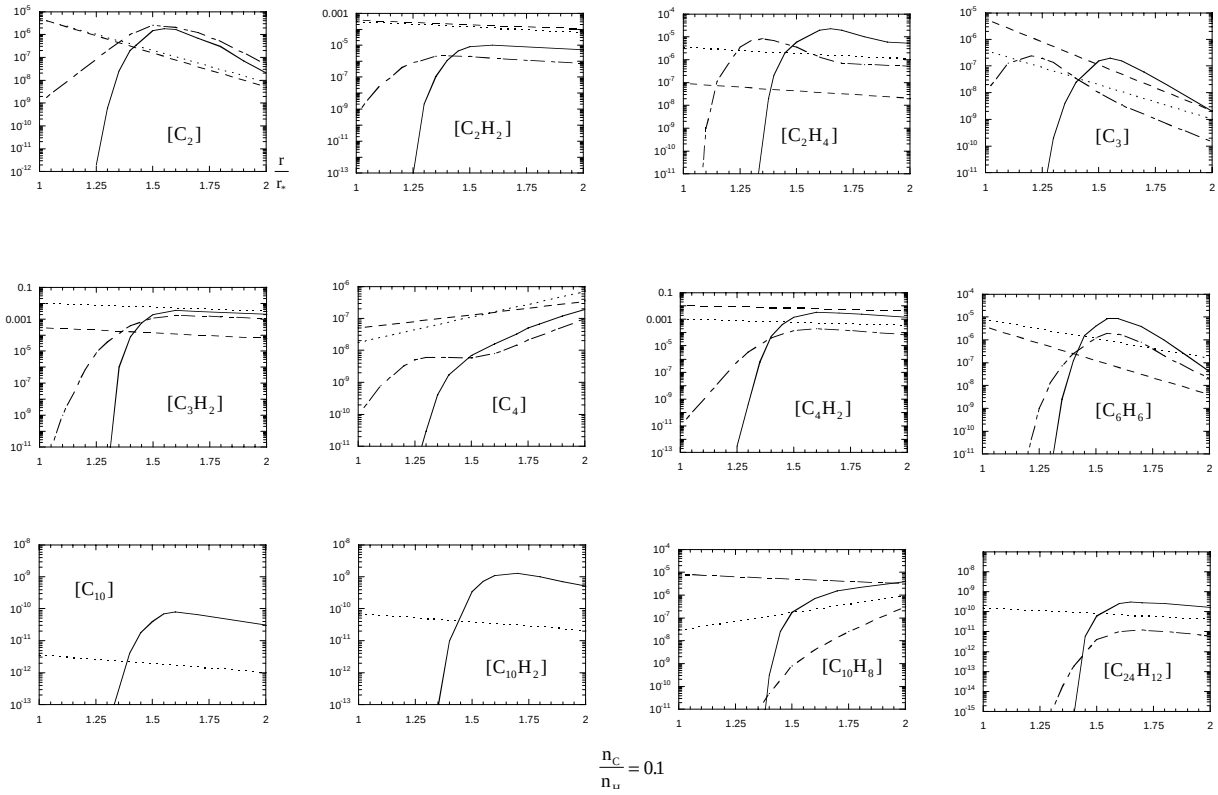

Fig. 4. Logarithmic abundances of some typical clusters when $\frac{n_C}{n_H} = 0.1$ vs. distance r ($r_* \sim 10^{13}$ cm) for $T_* = 2000$ K .....; 3000 K - - - - - -; 5000 K – – – – –; 7000 K _____.

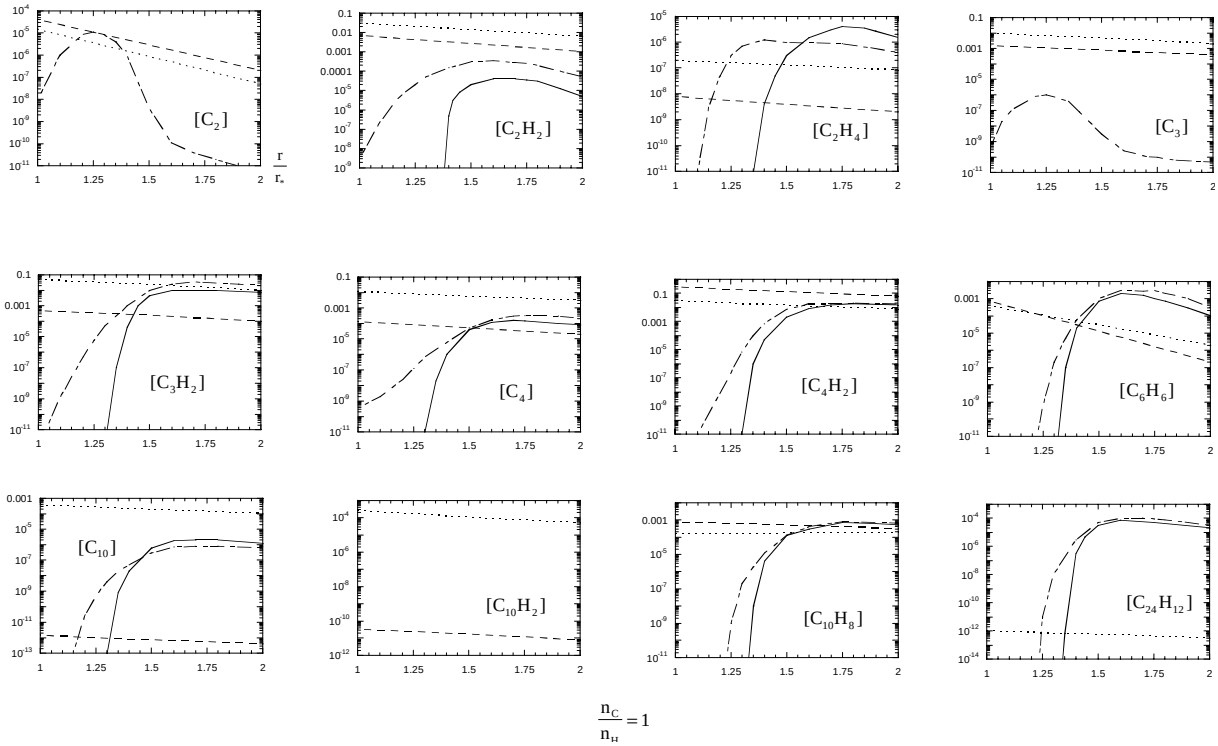

Fig. 5. Logarithmic abundances of some typical clusters when $\frac{n_C}{n_H} = 1$ vs. distance r ($r_* \sim 10^{13}$ cm) for $T_* = 2000$ K .....; 3000 K - - - - - -; 5000 K – – – – –; 7000 K _____.

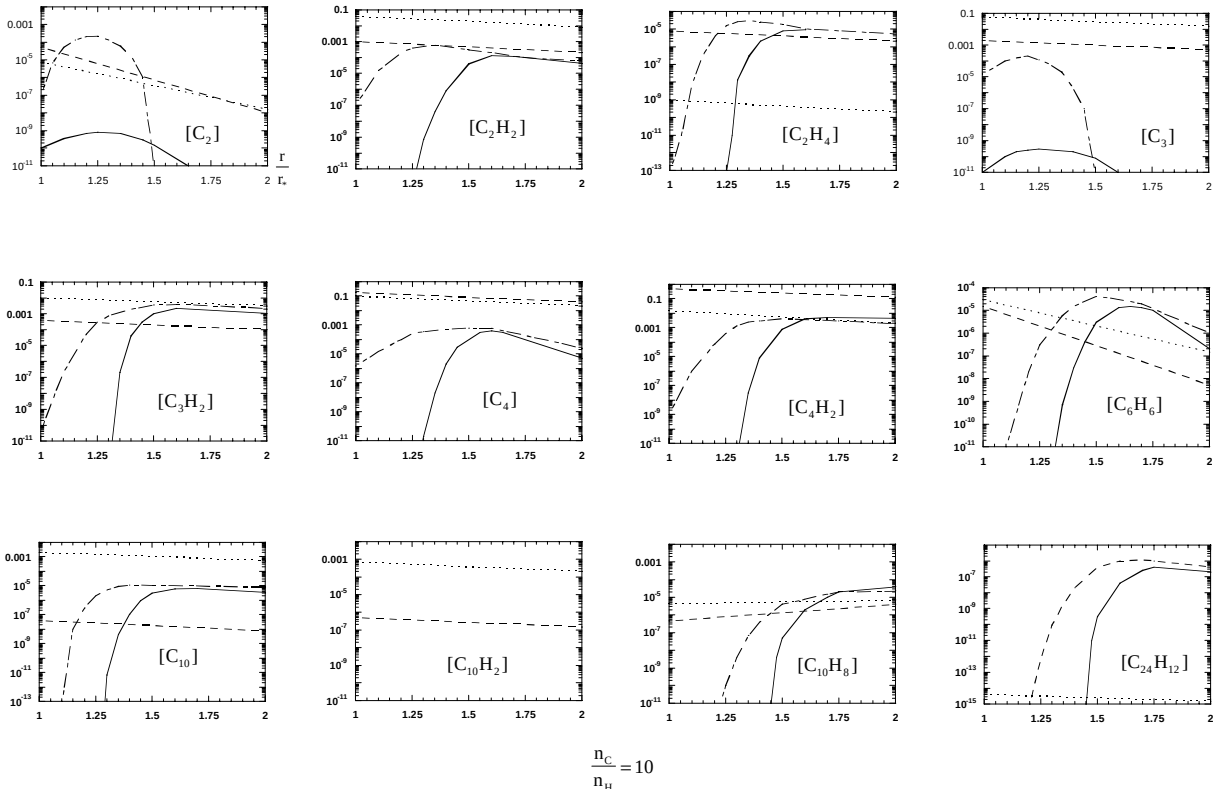

Fig. 6. Logarithmic abundances of some typical clusters when $\frac{n_C}{n_H} = 10$ vs. distance r ($r_* \sim 10^{13}$ cm) for $T_* = 2000$ K .....; 3000 K - - - - - -; 5000 K – – – – –; 7000 K _____.

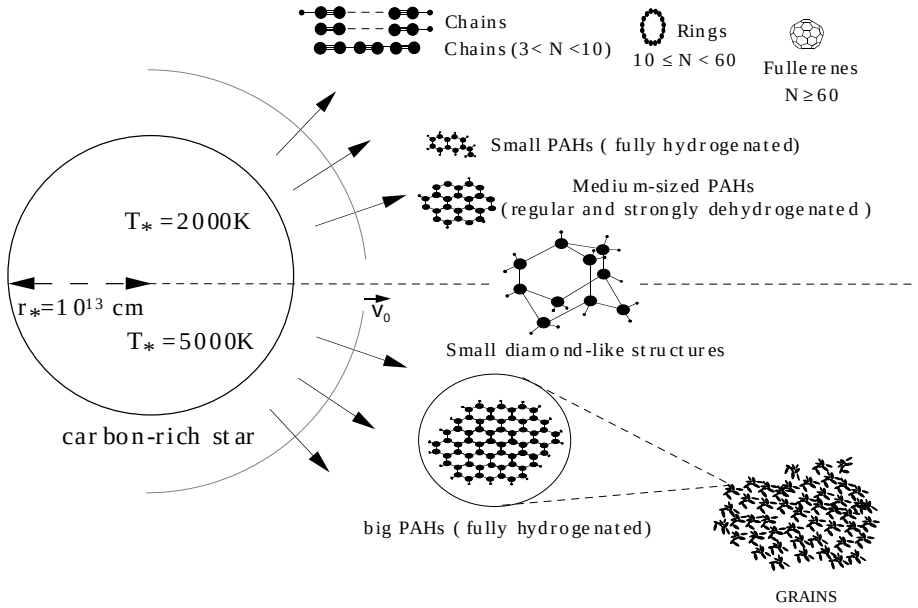

Fig. 7. Sketch of the carbon cluster distribution simulated in the outer atmosphere of a carbon-rich star at temperatures of 2000 and 5000 K for a carbon to hydrogen ratio of 1. The relative proportions of the various compounds are given in the text.

the form of a small piece of graphite. On the other hand, regular PAHs are more abundant than irregular congeners; for instance the coronene appears more abundant than its neighbours, $[\frac{C_{22}H_{12}}{C_{24}H_{12}}] \sim 0.02$. Likewise the abundance of medium-sized PAHs with a functional group attached to them is relatively low, $[\frac{C_{22}H_{11}-CH}{C_{24}H_{12}}] \sim 0.1$. The abundance of true PAHs is given in Fig. 9a, together with that of the dehydrogenated congeners (Fig. 9b). Summing up the abundances of true PAHs (regular and non-regular), of the corresponding species but dehydrogenated and of the intermediary forms gives the sp2 rate (Table 5a). Estimation of the sp2/sp ratio ($\sim 3\,10^{-2}$ for $\frac{n_C}{n_H} = 1$) shows that the aromatic-like compounds are not dominant compared to other forms of carbon, for instance the linear chains, C_nH and C_nH_2.

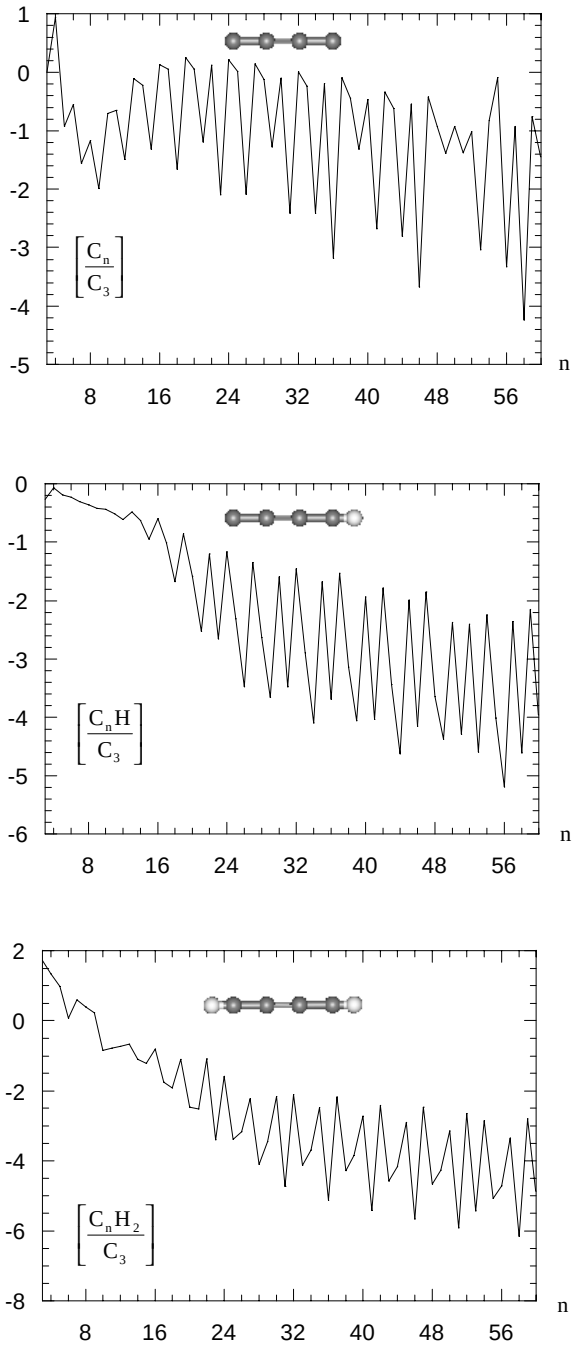

Fig. 8. Logarithmic abundances of C_n, C_nH and C_nH_2 linear species with respect to C_3 plotted as functions of r for $T_* = 2000\,K$ and $\frac{n_C}{n_H} = 1$.

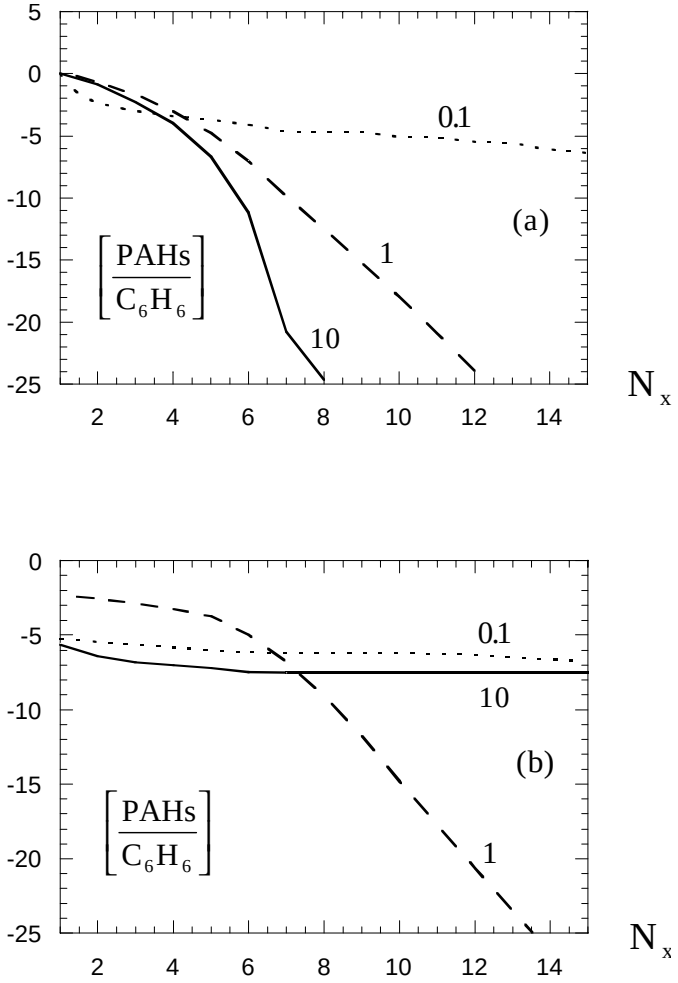

Fig. 9a and b. Logarithmic abundances of PAHs with respect to C_6H_6 plotted as functions of N_X (number of cycles) for $T_* = 2000\,K$ and various carbon to hydrogen ratios: $\frac{n_C}{n_H} = 0.1$, 1 and 10. **a** fully hydrogenated, **b** dehydrogenated to 50%.

The third type of carbon, sp3-hybridized, is stocked either in the form of linear (non-branched) alkanes when $N \leq 5$ or in the form of compact (diamond-like) compounds when $N \geq 6$. The sp3/sp ratio is of the order of 20 for $\frac{n_C}{n_H} = 0.1$ (Table 5b), indicating that sp3 could possibly compete with sp in the inner region of circumstellar envelopes. In fact, the sp-hybridized (acetylenic or cumulenic) structures are energetically the most stable ones, but tetrahedral (sp3) structures are in a sense globally less fragile [To dissociate a sp3-hybridized carbon at the periphery of any medium-sized carbon cluster, it is necessary to break two or three C C bonds against one bond in sp-hybridized open structures. This statement strongly contrasts with the population of clusters which very likely exists in the outer regions of circumstellar envelopes and in the interstellar medium, estimated to be essentially composed of sp2-hybridized structures (PAHs) (Allain et al. 1996a,b). But a simple scenario can still be envisaged in order to increase the sp2/sp ratio. As a matter of fact, clusters produced in the inner regions of circumstellar envelopes are very likely reprocessed by interstellar UV radiation field when driven in the outermost regions. As already noted above, the carbon chains are very floppy and can easily lead to small piece of graphite by structural rearrangement [Besides, the inverse process, leading from graphite to chain, is extremely difficult to realize].

However, more likely, small graphitic entities bound together by mono and di-acetylenic segments can also appear via this type of process, ultimately leading by gradual sticking to

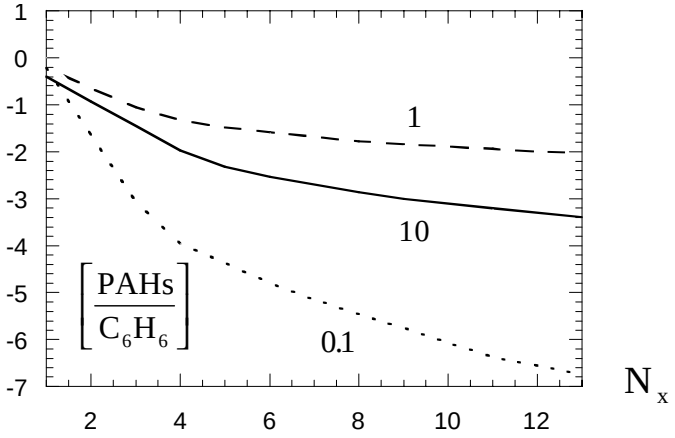

Fig. 10. Logarithmic abundances of fully hydrogenated PAHs with respect to C_6H_6 plotted as functions of N_X (number of cycles) for $T_* = 5000$ K and various carbon to hydrogen ratios: $\frac{n_C}{n_H} = 0.1$, 1 and 10.

Table 5a. $\frac{sp^2}{sp}$ ratio estimated for $\frac{n_C}{n_H} = 0.1, 1, 10$ at $T_* = 2000, 5000, 7000$ K

T_* (K)	2000	5000	7000
0.1	0.1	0.2	0.1
1	$2.6\,10^{-2}$	0.6	0.6
10	$9\,10^{-4}$	0.6	0.6

Table 5b. $\frac{sp^3}{sp}$ ratio estimated for $\frac{n_C}{n_H} = 0.1, 1, 10$ at $T_* = 2000, 5000, 7000$ K

T_* (K)	2000	5000	7000
0.1	22.0	39.1	8.2
1	$9\,10^{-3}$	0.3	0.3
10	$5\,10^{-5}$	$4\,10^{-3}$	0.6

a very intricate and strongly dehydrogenated network of mixed sp2 and sp hybridized carbons.

With regard to the diamond-like structures, we can also conjecture that these ones can be more and more dehydrogenated and graphitized when arriving in the outermost regions ($r \geq 100 r_*$) of the circumstellar envelope by interstellar UV radiation.

For $T_* = 3000$ K, we found $[\frac{C_3}{C_2}] \sim 10$ and $[\frac{C_2H_2}{C_2}] \sim 100$, both resulting from the fact that C_2 is fully hydrogenated in C_2H_2 (but $[\frac{C_2H_4}{C_2}] \sim 2\,10^{-4}$). On the other hand, $[\frac{C_3H}{C_3}] \sim 0.1$, $[\frac{C_3H_2}{C_3}] \sim 0.3$ indicating that C_3, weakly hydrogenated, is a free radical. But again as C_2, C_4 is fully hydrogenated, $[\frac{C_4}{C_4H_2}] \sim 5\,10^{-4}$. Carbon chains C_nH and C_nH_2 are very short, for instance $[\frac{C_{10}H}{C_3}] \sim 10^{-9}$ and $[\frac{C_{10}H_2}{C_3}] \sim 10^{-8}$. Temperatures ~ 3000 K are thus sufficient to impede the formation of linear C_nH and C_nH_2 species possessing a number of carbon atoms of the order of – or larger than – 10. Likewise monocyclic rings are not observed ($[\frac{C_{10}}{C_3}] \sim 10^{-8}$). Besides, benzene and naphtalene are abundant ($[\frac{C_6H_6}{C_2H_2}] \sim 0.1$, $[\frac{C_{10}H_8}{C_6H_6}] \sim 1$, but coronene is not present.

B/ $T_* = 5000 - 7000$ K

For moderately high temperatures, $\sim$ 5000–7000 K, typically corresponding to R Coronae Borealis stars (Schönberner, 1989), the scenario drastically changes. In the vicinity of the star, hydrogen and carbon largely remain in a atomic state. For instance, at $T_* = 5000$ K and $\frac{n_C}{n_H} = 1$, $[\frac{C_2}{C}] \sim 10^{-8}$, $[\frac{C_3}{C}] \sim 10^{-3}$, $[\frac{C_2H_2}{C_2}] \sim 0.1$. A very noticeable fact, however, is that as soon as self-shielding due to these clusters becomes efficient, formation and growth of medium-sized species appear very rapidly (Fig. 4-6) [As is well known, R CrB stars show deep minima in the light curves usually explained by formation of dust which blocks the photospheric flux very efficiently (Waters et al. 1990)]. Nevertheless, the compounds which are formed differ in a qualitative manner from those obtained at lower temperatures (2000 K). The linear chains are now very short ($[C_6H_2] \sim 10^{-5}$, but $[C_{10}H_2] \sim 10^{-15}$) even though monocyclic rings are still present, $[C_{10}] \sim 10^{-6} - 10^{-5}$. Larger values of n are not represented for the monocycles. Besides, benzene produced by isomerization of linear C_6 and subsequent hydrogenation is very abundant, $[C_6H_6] \sim 10^{-3}$ (even though gradually transformed into naphtalene by addition of C_4H_2). Then benzene and naphtalene act as nucleation points and promote formation of big PAHs by pumping of atomic carbon ($[C_{24}H_{12}] \sim 10^{-7} - 10^{-5}$). In clear contrast with the situation encountered in the low temperature regime (Fig. 10):

i/ PAHs are produced here at a very high rate ($[C_{24}H_{12}] \sim 10^{-5}$ against 10^{-10} at 2000 K).

ii/ these PAHs are generated in both regular and irregular – but compact – forms ($[\frac{C_{22}H_{12}}{C_{24}H_{12}}] \sim 1$ against 0.02 at 2000 K).

iii/ dehydrogenated PAHs are totally absent whereas at 2000 K dehydrogenated PAHs are dominant over fully hydrogenated species.

Furthermore, the very high sp2/sp ratio, of the order of 0.6 (Table 5a), shows that sp2 hybridized clusters (aromatic-like species) now compete with sp-hybridized species (linear chains and monocycles). Eventually nanodiamond-like structures are still present as noticed by the relatively high sp3/sp ratio (0.3).

The next stage is then to proceed from these medium-sized species, which are formed in the vicinity of the star over a fairly short distance $\leq r_*$, to microscopic grains ($\sim 0.01 - 0.1\,\mu$m in size). Very crude calculations show that medium-sized entities such as fully hydrogenated PAHs with 20–50 atoms can cluster together to generate microscopic grains over a distance of the order of $10 r_*$ [assuming an attractive potential of the order of several tenths of an eV; for coronene the calculated potential is 0.2–0.3 eV]. Following a very simple scenario, we obtain a hierarchy of clusters which gradually coagulate in order to produce very fluffy aggregates in which hydrogenated graphitic islands are loosely connected together by Van der Waals forces. These grains are surrounded by a relatively inert atmosphere composed of the most abundant species, that is C_4H_2. It is also likely that a few diacetylenic molecules and individual PAH units are loosely coupled to the carbonaceous particles in an exohedral position. On the other hand, both laboratory experiments and theoretical

arguments suggest that grains composed of more or less individualized structural units, the latter ones possessing relatively large optical gaps (~ 2.3 eV for coronene), are transparent in the visible. Besides, larger PAHs have comparatively smaller optical gaps making use of the relationship $\Delta E_{\rm gap} = \frac{6}{\sqrt{M}}$ (eV), where M is the number of rings in the structure (see Robertson 1991). At larger distances from the star, say when $r \geq 100 r_*$, the grains (formed in the innermost regions of the circumstellar envelope according to the present scenario) are UV-processed by the interstellar radiation. Consequently they become opaque in the visible by reduction of the optical gap due to dehydrogenation and subsequent graphitization (i.e. enlargement of the PAH structural units).

4. Conclusion

We have developed a multicomponent model of carbon cluster growth using reaction rate constants, deduced from combustion chemistry, geometrical parameters and dissociation energies as input data. The three forms of carbon, sp, sp2 and sp3 are simultaneously considered. In the framework of this mean field model a number of very efficient radicalar reactions are taken into account together with some other reactions involving an activation barrier. The calculations show that the distribution of carbon clusters in carbon-rich stellar atmospheres depends on the relative energetics of the clusters and on the kinetics of their growth. When the carbon to hydrogen abundance ratio is low, only small (non-condensable) molecules are formed in agreement with laboratory experiments on carbon vapour deposition. On the other hand, when this ratio is high (≥ 0.1), medium-sized species are produced of various types: carbon chains $\mathrm{C}_n\mathrm{H}$ or $\mathrm{C}_n\mathrm{H}_2$, carbon monocycles, C_n, and PAHs accompanied by their corresponding dehydrogenated congeners. At $T_* = 2000$ K, carbon chains or monocycles are clearly dominant over dehydrogenated (regular and relatively small) PAHs. In contrast, at $T_* = 5000$–7000 K, big (regular and irregular) PAHs are formed at much larger rate and compete with cumulenic structures.

References

Allain T., Leach S., Sedlmayr E., 1996a, A&A 305, 602
Allain T., Leach S., Sedlmayr E., 1996b, A&A 305, 616
Allamandola L.J., Tielens A.G.G.M., Barker J.R., 1989, ApJS 71, 733
Allen C.W., 1963, Astrophysical quantities. University of London: Athlone Press
Baulch D.L., Cobos C.J., Cox R.A., et al., 1992, J. Phys. Chem. Ref. Data 21,411
Cadwell B.J., Wang H., Feigelson E.D., Frenklach M., 1994, ApJ 429, 285
Cherchneff I.M., Barker J.R., Tielens A.G.G.M., 1992, ApJ 401, 269
Cherchneff I.M., Glassgold A.E., Mamon G.A.,1993, ApJ 410, 188
Cherchneff I.M., 1995, Ap&SS 224, 379
Freivogel P., Fulara J., Jakobi M., Forney D., Maier J.P., 1995, J.Chem. Phys. 103, 54
Frenklach M., Feigelson E.D., 1989, ApJ 341, 372
Frisch M.J., Trucks G.M., Schlegel H.B., et al., Gaussian 94, Revision C.3, Inc., Pittsburgh P.A. (1995)
Fye J.L., Jarrold M.F., 1997, J.Phys. Chem. A101,1836
Goeres A., Sedlmayr E., 1991, Chem. Phys. Lett. 184, 310
Habing H.J., 1996, A&A Rev 7, 97
Herbst E., 1991, ApJ 366,133
Hunter J.M., Fye J.L., Jarrold M.F., Roskamp E.J., 1994, In: Nenner I: (ed.) Molecules and Grains in Space, p571 (IAP Conference proceedings 312, New York)
Kerr T.H., Hibbins R.E., Miles J.R., et al., 1996, MNRAS 283, L105
Kiefer J.H., Mizerka L.J., Patel M.R., Wei H.C., 1985, J.Phys. Chem. 89, 2013
Knapp G.R. 1986, ApJ 311, 731
Krätschmer W., Lamb L.D., Fostiropoulos K., Huffman D.R., 1990, Nature 347,354
Krätschmer W., 1993, J. Chem. Soc. Faraday Trans. 89, 2285
Kroto H.W., Heath J.R., O'Brien S.C., Curl R.F., Smalley R.E, 1985, Nature 318,162
Kwok S. 1975, ApJ 198, 583
Léger A., Puget J.L., 1984, A&A 137,L5
Léger A. d'Hendecourt L., Défourneau D. 1989, A&A 216, 148
Merrill K.M., 1977, In: Kippenhahn R. (ed.) The Interaction of Variable Stars with their environments (Veroff. Remies Sternwarte, Bamberg, bd XI nº121, p. 446
Omont A., 1993, J. Chem. Soc. Faraday Trans. 89, 2137
Pascoli G., 1997, ApJ 489, 946
Pascoli G., Lavendy H., 1998a, Int. J. Mass Spectrom. Ion Proc. 173,41
Pascoli G., Lavendy H., 1998b, Int. J. Mass Spectrom. Ion Proc. 181,11
Reilman R.F., Manson S.T., 1979, ApJ 40, 815
Robertson J., 1991, Prog. Solid St. Chem. 21, 199
Salama F., Allamandola L.J., 1993, J.Chem. Soc. Faraday Trans. 89, 2777
Schönberner D., 1989, In: Johnson H.R., Zuckerman B. (eds.) Evolution of Peculiar Red Giant Stars, p. 348 (IAU colloquium 106, Bloomington)
Schröder D., Sülze D., Hrusak J., Böhme D., Schwarz H., 1991, Int. J. Mass Spectrom. Ion Proc. 110, 145
Sedlmayr E.,1990, In: Mennessier M.O., Omont O. (eds.) From Miras to Planetary Nebulae (Editions Frontières, p. 179)
Stein S.E., 1978, J. Chem. Phys. 82, 566
Thaddeus P., 1994, In: Nenner I. (ed.) Molecules and Grains in Space, p. 711 (IAP Conference proceedings 312, New York)
Tielens A.G.G.M., 1990, In: Menessier M.O., Omont O. (eds.) From Miras to Planetary Nebulae (Editions Frontières, p 186)
Tielens A.G.G.M. 1993, In: Millar T.J., Williams D.A. (eds.) Dust and Chemistry in Astronomy (Institute of Physics publishing, Bristol p103)
Tielens A.G.G.M., 1983, ApJ 271,702
Waters L.B.F.M., Waelkens C., Trams W.R., 1990, In: Menessier M.O., Omont O. (eds.) From Miras to Planetary Nebulae (Editions Frontières, p. 449)
Weltner W., Van Zee R.J., 1989, Chem. Rev. 89,1713
Williams D.A., 1994, In: Nenner I. (ed.) Molecules and Grains in Space, p. 3 (IAP Conference proceedings 312, New York)